ACS Macro Letters

Letter

pubs.acs.org/macroletters

Anisotropic Polymer Conformations in Aligned SWCNT/PS Nanocomposites

Wei-Shao Tung,[†] Russell J. Composto,[†] Nigel Clarke,[‡] and Karen I. Winey*[,†]

[†]Department of Materials Science and Engineering, University of Pennsylvania, Philadelphia 19104-6272, United States

[‡]Department of Physics and Astronomy, University of Sheffield, Sheffield S3 7RH, United Kingdom

Supporting Information

ABSTRACT: Polymer radii of gyration in isotropic single-walled carbon nanotube (SWCNT)/polymer nanocomposites were previously found to increase with increasing SWCNT concentration. Here, the SWCNTs in nanocomposites were aligned by melt fiber spinning, and the polymer chain conformations were found to be anisotropic. Using SAXS and SANS, the anisotropic SWCNT meshes were found to have smaller mesh sizes in the direction perpendicular to the alignment direction than along the alignment direction. At fixed SWCNT orientation, the radius of gyration was probed parallel and perpendicular to the alignment direction, R_g^{par} and R_g^{per}, respectively, using SANS. With increasing SWCNT concentration, R_g^{per} increases significantly more than R_g^{par}, such that the extent of anisotropy increases with SWCNT concentration. The anisotropic polymer conformation is larger in the direction perpendicular to the alignment direction, which corresponds to a smaller SWCNT mesh size. Thus, when the SWCNT concentration and alignment combine to produce a SWCNT mesh size that is smaller than the unperturbed R_g, the polymer conformation circumvents the SWCNTs by adopting a larger R_g. Changes in the polymer conformation in nanocomposites with rod-like nanoparticles has important ramifications for entanglement density, polymer dynamics, and mechanical properties.

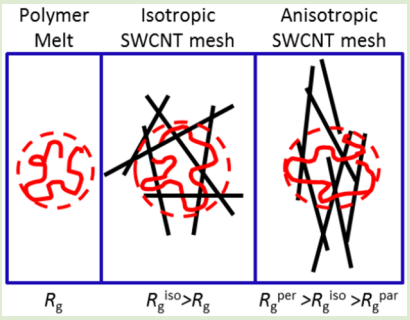

Nanoparticles with various functions, shapes, and sizes are incorporated into polymer matrices to form polymer nanocomposites with improved properties, including electrical, optical, mechanical, and flammability.[1−3] Adding nanoparticles to polymer matrices impact both structure and dynamics of the polymers. Given the interdependencies of polymer structure and dynamics, knowing how polymer conformations are affected by nanofillers provides insights to the observed changes in dynamics and further improves our ability to predict and design the properties of polymer nanocomposites. So far, most of the studies of how polymer structure is affected by nanofillers focuses on spherical nanoparticles (radius, r),[4−9] and it is concluded that the effect mainly depends on the polymer−nanoparticle interactions, size ratio of polymers (radius of gyration, R_g) to nanoparticles (R_g/r), and the spatial distribution of nanoparticles. It has been shown that nanoparticles smaller that R_g can serve as diluents, which can swell the polymer chains relative to the neat polymer in both experiments and simulations.[6,10]

Our previous study of isotropic carbon nanotube/polymer nanocomposites was the first experimental work investigating how polymer chains are affected by cylindrical nanofillers.[11] The polymer nanocomposites with single walled carbon nanotubes (SWCNTs) showed an increase in R_g with increasing SWCNT concentration, while R_g was independent of filler concentration in nanocomposites with multiwalled carbon nanotubes (MWCNTs). The diameters of the SWCNT bundles were smaller than the MWCNT bundles in these composites, so that at a fixed concentration the CNT mesh size was smaller for the SWCNT nanocomposites, and the polymer conformation adapted to this smaller mesh size by expanding. In this letter, we produce anisotropic SWCNT/polystyrene nanocomposites by melt fiber spinning, demonstrate that our annealing condition is sufficient to relax the polymers without disrupting the SWNCT alignment, characterize the extent of SWCNT alignment, and report the polymer radius of gyration at a constant degree of SWNCT orientation as a function of SWCNT concentration.

The SWCNT/polystyrene nanocomposites contain a mixture of polystyrene (PS, M_n = 117 kg/mol, PDI of 1.05) and deuterated polystyrene (dPS, M_n = 116 kg/mol, PDI of 1.03) with a volume ratio of dPS/hPS = 0.725/0.275 to minimize the scattering from the SWCNT by contrast matching and the interaction between dPS and hPS is negligible.[11] After characterizing the isotropic composites with SANS, they were melt extruded to align the SWCNTs, and different degrees of alignment were obtained by controlling the winder rate; see details in Supporting Information. The nanocomposite fibers were annealed (150 °C for 3 days) and then cut, arranged to maintain the extrusion direction, and compression molded into samples for SANS and SAXS. The 2D SANS data are anisotropic and the average intensities versus

Received: April 21, 2015
Accepted: August 10, 2015
Published: August 13, 2015

DOI: 10.1021/acsmacrolett.5b00256
ACS Macro Lett. 2015, 4, 916−920

q were obtained by integrating 25° (± 12.5°) over two orthogonal directions, namely, parallel and perpendicular to the extrusion direction, Figure 1a. This data reduction from 2D to

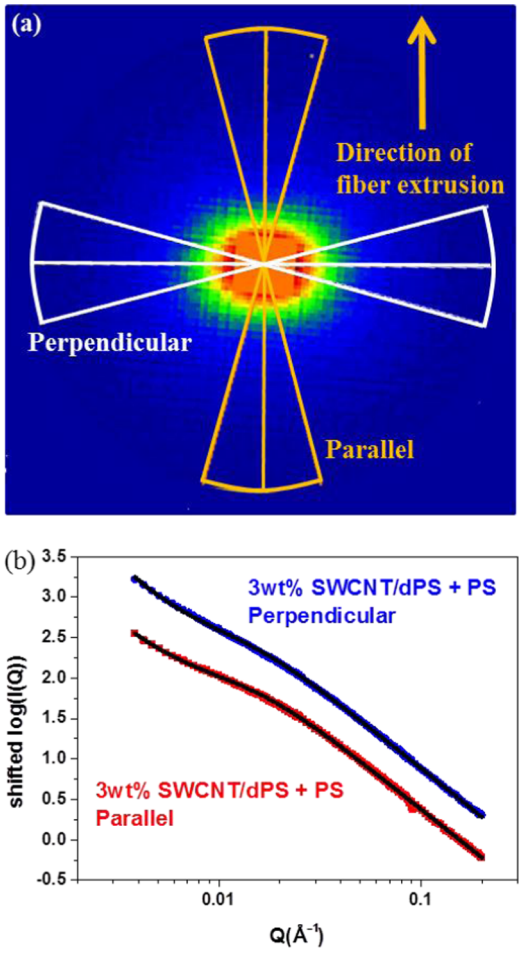

Figure 1. (a) SANS data (low q configuration) for an aligned 3 wt % SWCNT/dPS+PS nanocomposite. (b) $I(q)$ data from integrating over 25° parallel and perpendicular to the direction of alignment for SWCNTs. Black lines are best fits using eq 1. Data are shifted for clarity.

$I(q)$ data was applied for low and medium q ranges and subsequently combined, Figure 1b. The orthogonal integrations were also performed in the absence of anisotropy (i.e., dPS +PS) for comparison.

The $I(q)$ data were fit to a model developed in our previous work.[11] The scattering model includes contributions from polymer chain scattering, rod network scattering, and scattering from defects:

$$i(q) = A(1 - \Phi_{cnt}) \times \text{Debye}(q, R_g) + B \times q^{-2} + C \times q^{-4} \quad (1)$$

where

$$\text{Debye}(q, R_g) = \frac{2}{(qR_g)^4}[q^2R_g^2 - 1 + \exp(-q^2R_g^2)] \quad (2)$$

and R_g is the radius of gyration of polymer chains, and Φ_{cnt} denotes the volume fraction of SWCNTs. The Bq^{-2} term represents the rod network scattering derived from the scattering by a fractal object, which has a self-similar structure ($i(q) \sim q^{-D}$).[12] Here, D represents the fractal dimension, which has been shown to be ~2 for rod networks.[13,14] At very low q, the scattering intensity is dominated by voids and defects, as described by Porod's law,[15] with a q^{-4} dependence.

Melt fiber spinning elongates polymer conformations along the fiber axis (the direction of extensional flow) and these distorted conformations will persist indefinitely when the molten sample is rapidly cooled and held below the glass transition temperature. Thus, we first evaluate whether our annealing condition is sufficient to eliminate any chain distortions imposed by the extensional flow of fiber spinning. A dPS+PS blend was also melt fiber spun, annealed, and measured using SANS. The two data sets corresponding to parallel and perpendicular to the fiber axis were fit to eq 1. A was set as a shared fitting parameter, and Φ_{cnt} and B were set to zero, because there is no rod network in the homopolymer blend. The same R_g was obtained both perpendicular and parallel to the fiber extrusion direction (Figure S1), demonstrating that the annealing condition (150 °C for 3 days) is sufficient to remove anisotropic chain conformations produced by the melt extrusion. In addition, the R_g values from the annealed homopolymer sample (~9.4 nm) agreed with our previous study of compression molded and annealed samples.[11]

The parallel and perpendicular scattering profiles (q = 0.004 to 0.2 Å^{-1}) for the anisotropic SWCNT/dPS+PS nanocomposites with a particular SWCNT concentration were fit globally along with the scattering from the isotropic sample of the same nanocomposite and the homopolymer sample (dPS +PS). Specifically, A was set as a shared fitting parameter, Φ_{cnt} was set as a fixed parameter for the composites, and Φ_{cnt} = 0 for the homopolymer blend, and R_g^{par}, B_{par}, and C were set as free parameters for each data set. Each aligned SWCNT/dPS+PS sample provides values for B_{par}, B_{per}, R_g^{par}, and R_g^{per}. At each SWCNT concentration, this fitting approach also provides A, R_g^{par}, and R_g^{per} for the homopolymer blend and their values are in reasonable agreement from 0 to 10 wt % SWCNT (Figure S.2). An example of $I(q)$ for the 6 wt % SWCNT/dPS+hPS sample with isotropic and anisotropic SWCNT orientations is provided in Supporting Information (Figure S.3) to illustrate the difference in the scattering intensities. SANS data with fits to eq 1 are provided in Figure S.4, and an example showing how each of the components of the fit contributes to the overall fit is provided in Figure S.5.

The anisotropic SWCNT meshes in aligned SWCNT/dPS +PS samples were characterized using the Herman's orientation function (f_2).[16] Anisotropic 2D SAXS data was integrated from q = 0.01 to 0.12 Å^{-1} and plotted as a function of ϕ from 0° to 90°, where ϕ is the azimuthal angle between the fiber extrusion direction and the direction of the integrated intensity, Figure 2. When f_2 has the value of 1, 0, or −0.5, the SWCNTs are perfectly aligned perpendicular to the extrusion direction, the SWCNTs are isotropic, or the SWCNTs are perfectly aligned parallel to the extrusion direction, respectively. The SWCNT/dPS+PS nanocomposites studied here have f_2 values ranging from −0.02 to −0.14. Thus, although the annealing condition is sufficient for the dPS+PS matrix to relax, the SWCNTs remain aligned in the direction of extrusion.

Similar to the analysis of SANS (Figure 1), $I(q)$ from the SAXS data was obtained by integrating 25° (±12.5°) over the directions parallel and perpendicular to the extrusion direction. The X-ray scattering for polystyrene in this q range is relatively low, so that the scattering is dominated by the SWCNT networks arising from the electron density contrast between

DOI: 10.1021/acsmacrolett.5b00256
ACS Macro Lett. 2015, 4, 916−920

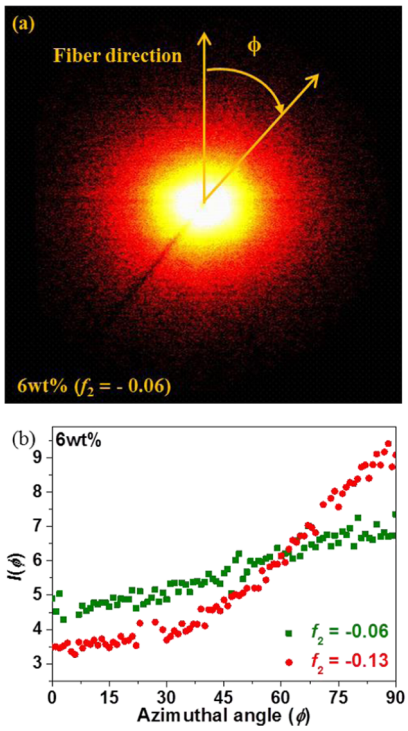

Figure 2. (a) SAXS data for an aligned 6 wt % SWCNT/dPS+PS nanocomposite with Herman's orientation parameter of −0.06. (b) $I(\phi)$ integrated from $q \sim 0.01$ to 0.12 Å^{-1} vs the azimuthal angle (ϕ) for the 6 wt % SWCNT/dPS+PS nanocomposite with different degrees of alignment (squares, $f_2 = -0.06$, and circles, $f_2 = -0.13$).

nanotubes and PS. Thus, for SAXS with q from 0.02 to 0.1 Å^{-1}, eq 1 simplifies to

$$i(q) = B \times q^{-n} \tag{3}$$

where n is ∼2 to 2.5. Figure 3a compares B_{per}/B_{par} obtained from SANS and SAXS for each sample with $-f_2$ from SAXS. In both scattering models, eqs 1 and 3, B represents the scattering strength of the rod networks, which is affected by the concentration of mesh sizes smaller than the probing length scale of the scattering experiments.[11] Theoretical work on anisotropic mesh sizes of rods distributed in 3D show that, at a fixed volume fraction of rods, the mean of mesh size parallel to the rod alignment direction is larger than the mean mesh size perpendicular to the rod alignment[17] (see Supporting Information). Figure 3b illustrates that an anisotropic SWCNT mesh has a higher concentration of SWNCTs within the probing length scale of the scattering experiments (green circle) perpendicular to the SWCNT alignment direction. Thus, $B_{per}/B_{par} > 1$ corresponds to SWCNT/dPS+PS nanocomposites with SWCNTs preferentially aligned along the fiber direction. As shown in Figure 3a, both SAXS and SANS values of B_{per}/B_{par} correlate well with $-f_2$, further supporting that larger values of B_{per}/B_{par} corresponds to greater SWCNT alignment. Finally, the extents of SWCNT alignment as measure by SANS and SAXS are in good agreement (Figure 3a).

Fitting eq 1 to SANS data also provides the radii of gyration parallel and perpendicular to the SWCNT alignment. Figure 4a plots R_g as a function of SWCNT concentration for the isotropic samples; these values are in good agreement with our early measurements of these samples.[11] Figure 4a also shows R_g^{par} and R_g^{per} for the anisotropic SWCNT/dPS+PS nano-

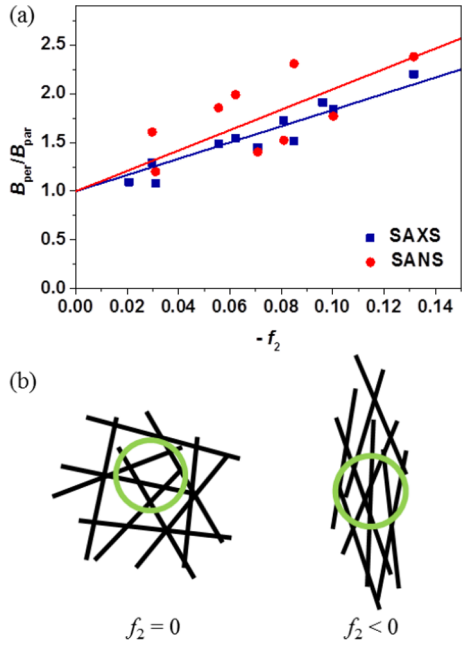

Figure 3. (a) B_{per}/B_{par} obtained from SANS and SAXS are plotted as a function of the Herman's orientation function from SAXS for aligned SWCNT/dPS+PS nanocomposites of various compositions. Lines are fits with a fixed intercept of 1 corresponding to isotropic samples. (b) Schematic of isotropic and aligned SWCNT rod networks, where the green circle represents the probing length scale of SANS and SAXS. The nanotube mesh is denser perpendicular to the extrusion direction than parallel.

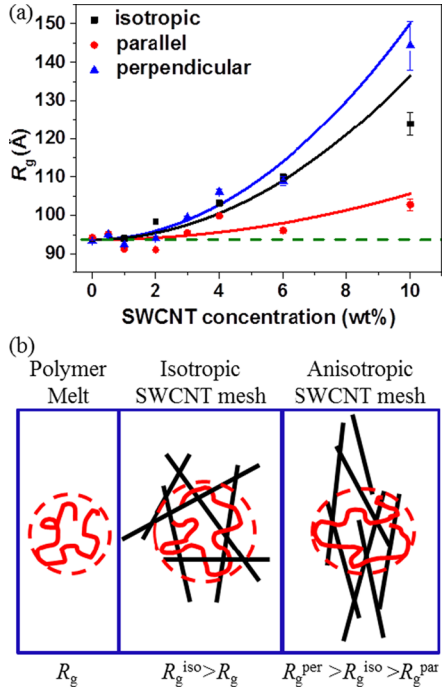

Figure 4. (a) Polymer radii of gyration in isotropic and aligned SWCNT/dPS+PS nanocomposites. The aligned nanocomposites have Herman's orientation function of −0.03 to −0.08. Lines are guides to the eye. (b) Schematic illustration of polymer chains in polymer melt with bulk R_g, in isotropic nanocomposites with isotropic expansion (R_g^{iso}), and in anisotropic nanocomposites with anisotropic expansion ($R_g^{per} > R_g^{par}$).

DOI: 10.1021/acsmacrolett.5b00256
ACS Macro Lett. 2015, 4, 916−920

composites, with $-f_2 = -0.03$ to -0.08. This range of $-f_2$ was selected to provide the widest range in SWCNT concentration at comparable SWCNT alignment. Compared to R_g in isotropic nanocomposites, R_g^{per} is slightly higher, while R_g^{par} is substantially lower and even close to the bulk R_g. This indicates that the polymer chain expands perpendicular to the direction of SWCNTs, as shown schematically in Figure 4b. In contrast, if there were strong attractions between the polymer and the SWCNTs, one would expect the polymer conformation to be extended along the SWCNT direction; thus, Figure 4a confirms that interactions between nanotubes and polystyrene are weak.

The nanotube mesh size in nanotube/PS nanocomposites dictates the radius of gyration of PS. In isotropic SWCNT/dPS +PS nanocomposites, the distribution of mesh sizes shifts to smaller values with increasing SWCNT concentration and the measurable size range is a few nanometers to tens or hundreds of nanometers.[11] When the mesh size is smaller than the bulk polymer conformation ($R_g \sim 9.50 \pm 0.03$ nm),[11] polymer conformations expand to circumvent the SWCNTs. Note that the diameter of the SWCNT bundles is smaller than R_g, so the polymers circumvent the nanoparticles with minimal entropic penalty; this is quite distinct from being confined between impenetrable walls. When the SWCNTs are isotropic, the chain expansion is isotropic because the SWCNT mesh size is isotropic. When the SWCNTs are aligned, the mesh sizes perpendicular to the direction of alignment are smaller, so polymer chains preferentially expand perpendicular to the SWNCT alignment. The effect becomes more pronounced at higher SWCNT concentrations. In contrast, parallel to the SWCNT alignment, the mesh size increases with alignment and R_g^{par} is smaller than R_g^{per} and R_g^{iso}. The anisotropic R_g found in these anisotropic nanotube/PS nanocomposites is not directly the result of anisotropic nanoparticles, but rather the ability of macroscopic processing to form anisotropic nanoscale assemblies of nanoparticles. If spherical nanoparticles were processed to form an anisotropic and nanoscale assembly in polymer nanocomposites, perhaps due to chaining effects under flow, then an anisotropic polymer conformation would be expected.

In conclusion, SWCNT/dPS+PS nanocomposites with 0−10 wt % SWCNT were extruded, annealed, and characterized by SANS and SAXS. The ratio between the scattering strength of SWCNT networks perpendicular and parallel to the alignment direction of SWCNTs (B_{per}/B_{par}) is well correlated to the Herman's orientation function. The orientation parameter was then used to select a set of nanocomposites with comparable SWCNT alignment to investigate the polymer conformation as a function of SWCNT concentration. Above ∼5 wt % SWCNT, polymer chains experience smaller mesh sizes perpendicular to the alignment direction and adopt an expanded chain conformation to circumvent the SWCNTs. Simultaneously, polymer chains experience larger mesh sizes parallel to the alignment direction and adopt less expanded chain conformations to produce anisotropic polymer conformations with $R_g^{per} > R_g^{par}$. Interestingly, this finding demonstrates that these SWCNTs and PS are not strongly attractive, which would be expected to produce the opposite effect on chain conformations, namely, $R_g^{per} < R_g^{par}$. As more cylindrical nanoparticles become available, polymer conformations should be explored across a wider range of nanoparticles size (diameter, length), nanoparticle mesh size (as controlled by nanoparticle size, concentration, and alignment), and polymer size (radius of gyration), as well as investigating systems with favorable nanoparticle−polymer interactions.

■ ASSOCIATED CONTENT

Supporting Information

The Supporting Information is available free of charge on the ACS Publications website at DOI: 10.1021/acsmacrolett.5b00256.

Sample preparation, experimental details, fitting results, and a theoretical analysis of mesh size for anisotropic rod networks (PDF)

■ AUTHOR INFORMATION

Corresponding Author

*E-mail: winey@seas.upenn.edu. Fax: 215-573-2128.

Notes

The authors declare no competing financial interest.

■ ACKNOWLEDGMENTS

This work is mainly funded by the National Science Foundation DMR-12-10379 (W.-S.T., K.I.W. and R.J.C.) and EPSRC EP/G065373/2 and EP/J018503 (N.C.). The authors acknowledge the support of the National Institute of Standards and Technology, U.S. Department of Commerce, in providing the neutron research facilities used in this work. The authors thank Dr. Yun Liu and Dr. Boualem Hammouda of NIST for assisting with SANS experiments, and this work utilized facilities supported in part by the National Science Foundation under Agreement No. DMR-0944772. The authors also thank Han-Chang Yang for assistance with the MAXS facility at the Laboratory for Research on the Structure of Matter at the University of Pennsylvania, which is funded in part by the MRSEC Program of the National Science Foundation (DMR 11-20901). Partial support also provided by NSF DMR 09-07493.

■ REFERENCES

(1) Alexandre, M.; Dubois, P. *Mater. Sci. Eng., R* **2000**, *28* (1−2), 1−63.

(2) Balazs, A. C.; Emrick, T.; Russell, T. P. *Science* **2006**, *314* (5802), 1107−1110.

(3) Coleman, J. N.; Khan, U.; Gun'ko, Y. K. *Adv. Mater.* **2006**, *18* (6), 689−706.

(4) Nakatani, A. I.; Chen, W.; Schmidt, R. G.; Gordon, G. V.; Han, C. C. *Int. J. Thermophys.* **2002**, *23* (1), 199−209.

(5) Sen, S.; Xie, Y. P.; Kumar, S. K.; Yang, H. C.; Bansal, A.; Ho, D. L.; Hall, L.; Hooper, J. B.; Schweizer, K. S. *Phys. Rev. Lett.* **2007**, *98* (12), 128302.

(6) Tuteja, A.; Duxbury, P. M.; Mackay, M. E. *Phys. Rev. Lett.* **2008**, *100* (7), 077801.

(7) Jouault, N.; Dalmas, F.; Said, S.; Di Cola, E.; Schweins, R.; Jestin, J.; Boue, F. *Macromolecules* **2010**, *43* (23), 9881−9891.

(8) Nusser, K.; Neueder, S.; Schneider, G. J.; Meyer, M.; Pyckhout-Hintzen, W.; Willner, L.; Radulescu, A.; Richter, D. *Macromolecules* **2010**, *43* (23), 9837−9847.

(9) Crawford, M. K.; Smalley, R. J.; Cohen, G.; Hogan, B.; Wood, B.; Kumar, S. K.; Melnichenko, Y. B.; He, L.; Guise, W.; Hammouda, B. *Phys. Rev. Lett.* **2013**, *110* (19), 196001.

(10) Frischknecht, A. L.; McGarrity, E. S.; Mackay, M. E. *J. Chem. Phys.* **2010**, *132* (20), 204901.

(11) Tung, W. S.; Bird, V.; Composto, R. J.; Clarke, N.; Winey, K. I. *Macromolecules* **2013**, *46* (13), 5345−5354.

(12) Teixeira, J. *J. Appl. Crystallogr.* **1988**, *21*, 781−785.

DOI: 10.1021/acsmacrolett.5b00256
ACS Macro Lett. 2015, 4, 916−920

(13) Schaefer, D. W.; Zhao, J.; Brown, J. M.; Anderson, D. P.; Tomlin, D. W. *Chem. Phys. Lett.* **2003**, *375* (3−4), 369−375.
(14) Zhou, W.; Islam, M. F.; Wang, H.; Ho, D. L.; Yodh, A. G.; Winey, K. I.; Fischer, J. E. *Chem. Phys. Lett.* **2004**, *384* (1−3), 185−189.
(15) Debye, P.; Anderson, H. R.; Brumberger, H. *J. Appl. Phys.* **1957**, *28* (6), 679−683.
(16) Klug, H. P., Alexander, L. E. *X-ray Diffraction Procedures: For Polycrystalline and Amorphous Materials*, 2nd ed.; Wiley-Interscience: New York, 1974.
(17) Pan, N. *J. Compos. Mater.* **1994**, *28* (16), 1500−1531.

DOI: 10.1021/acsmacrolett.5b00256
ACS Macro Lett. 2015, 4, 916−920